ISSN 1061-933X, Colloid Journal, 2018, Vol. 80, No. 2, pp. 167–183. © Pleiades Publishing, Ltd., 2018.
Original Russian Text © G.G. Kodenev, 2018, published in Kolloidnyi Zhurnal, 2018, Vol. 80, No. 2, pp. 177–193.

The Rate of Spontaneous Formation of Microscopic Nuclei in Supersaturated Vapor

G. G. Kodenev

Multichrom Ltd., Novosibirsk, 630117 Russia

e-mail: root@multichrom.nsk.ru

Received August 4, 2017

Abstract—The equilibrium nucleus-size distribution determined by the method of statistical physics has been analyzed. The analysis has shown that nuclei composed of 1000 or fewer molecules are microscopic objects. They are described by partition functions and cannot be described by thermodynamic methods. An approach has been proposed that makes it possible to determine a partition function over internal degrees of freedom of a nucleus and express the aforementioned distribution via commonly accepted thermodynamic parameters. The solution of the problem is reduced to the determination of the evaporation rate of clusters by extrapolating the evaporation rate, which has been calculated for a macroscopic droplet of an incompressible liquid in terms of thermodynamic concepts with allowance for fluctuations, to the sizes of nuclei. As a result, a theory has been formulated for homogeneous stationary nucleation. The comparison of the proposed theory with experimental data has shown that the calculated sizes of critical nuclei coincide with the measured ones and that the theoretical nucleation rates either coincide with the measured rates or agree with them within one or two decimal orders of magnitude.

DOI: 10.1134/S1061933X18020047

INTRODUCTION

Nucleation of a new liquid phase in a supersaturated vapor is the first stage, which, to a great extent, determines the total rate of condensation. The classical theory of the stationary isothermal nucleation, which was formulated almost a century ago by Folmer and Veber [1], Becker and Döring [2], and Zel'dovich [3], has, up to the present, been most widely used for the prediction and qualitative and quantitative description of this phenomenon. According to the classical theory, nuclei are quiescent and nonrotating spherical droplets possessing all the properties of a macroscopic liquid, while their size is only a few times larger than the sizes of individual molecules. However, the improvement of experimental equipment and methods has resulted in finding that the classical nucleation theory (CNT) is not quite true. In some cases, the differences between the measured and predicted nucleation rates reach five to seven decimal orders of magnitude. In the opinion of Lothe and Pound [4], the incorrectness of the CNT is associated with "assigning macroscopic thermodynamic properties to the critical nuclei, a practice which is permissible for sufficiently large nuclei but constitutes a dangerous assumption in dealing with small clusters of the order of 100 molecules" or less. The aforementioned researchers [4], Frenkel' [5], and their successors [6–15] made a great effort to take into account the microscopic character of nuclei, thereby improving the nucleation theory. They did not refuse to engage in a thermodynamic consideration of nuclei, but rather preferred to introduce various microscopic corrections into the free energy of nuclei depending on the consideration of a nucleus: e.g., it may be considered to be a "macromolecule" subjected to thermal motion or a volume, which is "cut" out of a bulk liquid, is bounded by rigid walls, and has a fluctuating center of mass, etc. However, the variants of the nucleation theory elaborated in this way have not improved the relationship between the theoretical and experimental data as a whole. Moreover, the question remains open as to the relation between the corrected "free energies" of nuclei and the true free energy of droplets composed of large numbers (on the order of 10^{20}) of molecules, and whether they possess all the properties of real free energy.

In this work, another approach, which has been partly described elsewhere [16, 17], has been proposed. The approach is based on the nucleus-size distribution in a supersaturated vapor, following from statistical physics, which, in the opinion of Zel'dovich [3], may be used to solve the problem of nucleation. The analysis of the distribution has led to the conclusion that clusters containing less than 1000 molecules are microscopic objects and, therefore, cannot be described by thermodynamic potentials, but rather are characterized by their partition functions. A method has been described, which makes it possible to express

the nucleus-size distribution via experimentally measured degree of supersaturation (hereafter, supersaturation) and temperature. It has been shown that, in order to find required partition functions, it is necessary to know the evaporation rate of nuclei as depending on their sizes. It is supposed that the difference between the evaporation rates of real nuclei and similar classical droplets is due to fluctuations of their parameters. The evaporation rate of macroscopic droplets has been calculated taking into account the corrections for the fluctuations in their shapes and temperatures. The evaporation rate of clusters is determined by extrapolating the obtained dependences to the sizes of nuclei. The nucleus-size distribution and the rate of stationary isothermal nucleation have been calculated and compared with new and/or refined experimental data and predictions of the CNT.

1. ON APPLICABILITY OF THERMODYNAMICS TO NUCLEUS CLUSTERS

Let us consider the metastable state of a supersaturated vapor as an equilibrium mixture of interacting gases occurring at constant temperature T and pressure P following Frenkel' [5]. Assume that clusters consisting of g molecules compose a gas of some type in the mixture, i.e., a gas of g-mers, A_g. The following elementary reactions proceed in a system with volume V_s:

$$\begin{aligned} &A_1 + A_1 = A_2 \qquad A_{g-1} + A_1 = A_g \\ &A_2 + A_1 = A_3 \qquad \cdots\cdots\cdots\cdots \\ &\cdots\cdots\cdots\cdots \qquad A_{G-1} + A_1 = A_G \qquad A_G \to GA_1. \end{aligned}$$

The equilibrium in such a mixture is characterized by the following set of equations [18]:

$$\mu_g = g\mu_1, \quad 2 \le g \le G, \tag{1}$$

where μ_1 and μ_g are the chemical potentials of the gases consisting of monomers and g-mers, respectively. Substituting the values of the chemical potentials of the gases $\mu_g(P_g,T) = kT\ln(P_g/P_0) + \chi_g(T)$ into set (1) and considering the gases to be ideal, we obtain partial pressure P_g and number density n_g of g-mers in the mixture:

$$\begin{aligned} P_g &= P_0 \exp\left[\frac{g\mu_1 - \chi_g(T)}{kT}\right] \\ \text{and } n_g &= \frac{P_0}{kT}\exp\left[\frac{g\mu_1 - \chi_g(T)}{kT}\right]. \end{aligned} \tag{2}$$

Here, k is the Boltzmann constant and $\chi_g(T) = -kT\ln\left(\frac{kT}{V_sP_0}Z_g\right)$ is the pressure-independent component of chemical potential $\mu_g(P_g, T)$, where Z_g is the partition function over all degrees of freedom of a g-mer and P_0 is the pressure equal to one unit of pressure; e.g., in the CGS system of units, $P_0 = 1$ dyne/cm^2. Pressure P_0 has been introduced to avoid the presence of dimensional functions under the logarithm. Analogously to polyatomic gases, the $\chi_g(T)$ function may be represented as a sum of terms corresponding to translational $\chi_g^{(t)}(T)$, rotational $\chi_g^{(r)}(T)$, and vibrational $\chi_g^{(v)}(T)$ degrees of freedom: $\chi_g(T) = \chi_g^{(t)}(T) + \chi_g^{(r)}(T) + \chi_g^{(v)}(T)$. Taking this into account, we, from relations (2), obtain the following:

$$n_g = \frac{P_0}{kT}\exp\left[-\frac{\chi_g^{(t)} + \chi_g^{(r)}}{kT}\right]\exp\left[\frac{g\mu_1 - \chi_g^{(v)}}{kT}\right]. \tag{3}$$

Substituting $\chi_g^{(t)}(T)$ and $\chi_g^{(r)}$ in the explicit form,

$$\begin{aligned} \chi_g^{(t)} &= -kT\ln\left[\frac{kT}{V_sP_0}Z_g^{(t)}\right] \\ &= -kT\ln\left[\frac{kT}{P_0}\left(\frac{mgkT}{2\pi\hbar^2}\right)^{3/2}\right], \end{aligned} \tag{3a}$$

$$\chi_g^{(r)} = -kT\ln Z_g^{(r)} = -kT\ln\left[\frac{(2kT)^{3/2}(\pi I_g^3)^{1/2}}{\gamma_g\hbar^3}\right],$$

where m is the mass of a molecule; $Z_g^{(t)}$ and $Z_g^{(r)}$ are the translational and rotational partition functions of a g-mer, respectively; $\hbar$ is the Planck constant; $I_g^3 = I_{g,x}I_{g,y}I_{g,z}$ is the product of principal moments of inertia, which are assumed to be the same for a liquid cluster; and γ_g is the symmetry number of a g-mer, we arrive at

$$n_g = \left(\frac{mgkT}{2\pi\hbar^2}\right)^{3/2}\frac{(2kT)^{3/2}\left(\pi I_g^3\right)^{1/2}}{\gamma_g\hbar^3}\exp\left(\frac{g\mu_1 - \chi_g^{(v)}}{kT}\right). \tag{4}$$

Expression (4), as well as equivalent relations derived by Band [19] $N_g = Z_g\exp\left(\frac{g\mu_1}{kT}\right)$ and Frenkel' [5] $N_g = \frac{N_1^gZ_g}{Z_1^g}$, where $N_g = n_gV_s$ and $N_1 = n_1V_s$ are the equilibrium numbers of clusters and molecules of a vapor in a system, is used to solve a problem relevant to the determination of the size distribution of nucleus clusters (g-mers), when it is possible to calculate the $\chi_g^{(v)} = -kT\ln Z_g^{(v)}$ function, where $Z_g^{(v)}$ is the partition function over the vibrational degrees of freedom of a g-mer, and relate the obtained distribution to the experimentally measured supersaturation. Commonly, this is performed using the so-called "replacement procedure" [9–13], which consists in the use of formulas relating free energy F_g to the partition functions of a nucleus as follows:

$$F_g = -kT\ln Z_g = \chi_g(T) + kT\ln(kT/V_sP_0)$$
$$\text{and } F_g = -kT\ln Z_g^{(v)} = \chi_g^{(v)}(T). \quad (5a)$$

The determination of the exponential term in Eq. (2) or (4), respectively, is then reduced to calculating the work of g-mer formation from g bulk liquid phase molecules. The use of the replacement procedure (relations (5a)) to nuclei is generally accepted and, at the same time, disputed. For example, Dillmann and Meier [14] used the former of the relations, while Frenkel' [5] and Lothe and Pound [4] employed the latter. In the macroscopic limiting case $g \to \infty$, in which relations (5a) are valid, the free energy of a droplet is represented by the sum of the bulk and surface terms: $F_g = f_\infty g + \alpha g^{2/3}$, where f_∞ is the free energy as calculated per a liquid molecule, and $\alpha = 4\pi\sigma(3v/4\pi)^{2/3}$, where σ and v are the surface tension and the volume of a liquid molecule, respectively. Here, the free energy may also be equated to the sums of functions $\chi_g^{(v)} + \chi_g^{(t)} + kT\ln(kT/V_sP_0)$ and $\chi_g^{(v)} + \chi_g^{(r)}$:

$$F_g = f_\infty g + \alpha g^{2/3} = \chi_g^{(v)} + \chi_g^{(t)}$$
$$+ kT\ln(kT/V_sP_0) = \chi_g^{(v)} + \chi_g^{(r)}. \quad (5b)$$

It is worth noting that almost all relations (5) with different replacement factors were used to specify the free energy of a nucleus in the course of the aforementioned discussion of the definition of a nucleus [5–15].

Why is the free energy of a droplet introduced so ambiguously? The contributions from three or six external degrees of freedom to the free energy of a droplet are negligible as compared with the contribution from a huge number (on the order of 10^{20}–10^{23}) of vibrational degrees of freedom; therefore, all relations (5) are exact. The free energy of a macroscopic droplet is unambiguously determined by any of equalities (5). However, the situation fundamentally changes upon decreasing the number of molecules in a droplet. The free energy rapidly decreases in accordance with a power law, while contributions $\chi_g^{(t)}$ and $\chi_g^{(r)}$ of external degrees of freedom, which are in a logarithmic dependence on g, decrease very slowly; therefore, their relative fractions in the free energies determined by expressions (5) increase. When the number of molecules in a droplet becomes so small that the contribution from the external degrees of freedom becomes comparable with the free energy, the values of the latter calculated by different relations (5) become unequal to each other. The distortion of the relations suggests that the object has become microscopic. Thus, by comparing the contribution from the external degrees of freedom $\chi_g^{(t)} + \chi_g^{(r)} + kT\ln(kT/V_sP_0)$ with the surface term of the free energy $\alpha g^{2/3}$, which varies most slowly, we may determine the region of applicability of thermodynamics to the problem of nucleation. This contribution turns out to be equal to $(0.00045–0.0018)\alpha g^{2/3}$ at $g = 10^6$, nearly $(0.008–0.034)\alpha g^{2/3}$ at $g = 10^4$, $(0.035–0.14)\alpha g^{2/3}$ at $g = 10^3$, and comparable with the value of $\alpha g^{2/3}$ at smaller sizes of a nucleus, at which thermodynamics is obviously inapplicable.

The explicit forms of the $\chi_g^{(t)}$ and $\chi_g^{(r)}$ functions (3a), as well as the fact that, for the majority of the studied liquids, the value of α is equal to $(7–30)kT$, were used when performing the estimations. It was assumed that $V_s = 1$. When calculating the rotational partition function, and the moments of inertia of clusters were taken to be equal to the moments of inertia of droplets having the density of an ordinary liquid.

Finally, let us determine the effect of the replacement procedure on number density n_g of nuclei. Initially, we replace the $\chi_g^{(v)}$ function, which takes into account only the internal degrees of freedom, by the free energy in Eq. (4), as Frenkel' [5] and Lothe and Pound [4] did. Then, let us replace the χ_g function that corresponds to the total partition function by the same free energy in Eqs. (2) according to relations (5a), as Dillmann and Meier did in [14], and compare the obtained results. It has appeared that, in the first case, the number density of nuclei is a huge number of times ($\approx 10^{30}g^4$) higher than that obtained in the second case. For the spontaneous nucleation of supersaturated water vapor, this difference amounts to nearly 10^{38}. Note that the effect of the replacement procedure underlies the Lothe–Pound paradox. Comparison between number density n_g determined in the first case by Eq. (4) and the prediction of CNT, which differs from the second case in the presence of factor $n_1 \approx 10^{18}$, shows that the difference, with allowance for the factor of the replacement, is 17 decimal orders of magnitude.

To complete the discussion of this question, it should be recollected once more that the nuclei with which experimenters work are composed of a hundred or fewer molecules and are microscopic objects. Therefore, the only correct method for solving the problem of nucleation consists in the direct determination of the $\chi_g^{(v)}$ or χ_g function.

2. EQUILIBRIUM NUCLEUS-SIZE DISTRIBUTION

In this work, we calculate the nucleus-size distribution and the nucleation rate via the well-known physicochemical characteristics of substances by calculating the $\chi_g^{(v)}(T)$ function determined at all $g \geq 1$. We shall search for this function in the following form:

$$\chi_g^{(v)}(T) = f_\infty g + ag^{2/3} + f(g) + C$$
$$= g\mu_{liq} - P_\infty vg + ag^{2/3} + f(g) + C. \quad (6)$$

Here, $\mu_{liq}(T)$ is the chemical potential of a liquid, P_∞ is the saturation pressure of a vapor over a planar liquid surface, $f(g)$ is some correction function, and C is a g-independent constant. This representation of the $\chi_g^{(v)}(T)$ function is quite reasonable. In the macroscopic limiting case, at $g \to \infty$, $\chi_g^{(v)}(T)$ is, by definition, the macroscopic-droplet free energy, which is, as usual, equal to $f_\infty g + \alpha g^{2/3} = g\mu_{liq} - P_\infty v g + \alpha g^{2/3}$. Correction function $f(g)$ is selected in such a manner that it is negligible at $g \to \infty$, $\lim[f(g)/g^{2/3}] = 0$, and, in addition to constant C, ensures the fulfillment of equality (6) at low g values. For now, we shall not consider the question as to the form of the $f(g)$ function, but rather determine constant C. For this purpose, let us take advantage of the fact that, at $g = 1$, the $\chi_g^{(v)}(T)$ function is equal to the vibrational component of vapor chemical potential $\chi_1^{(v)}$. From this,

$$C = \chi_1^{(v)}(T) - \mu_{liq} - \alpha - f(1) + P_\infty v. \quad (7)$$

Substituting Eq. (7) into Eq. (6), we obtain

$$\chi_g^{(v)}(T) = \mu_{liq}(g-1) + \alpha(g^{2/3} - 1) - P_\infty v(g-1) + f(g) - f(1) + \chi_1^{(v)}(T). \quad (8)$$

The determination of constant C in Eq. (7) has enabled us to "bind" the $\chi_g^{(v)}(T)$ function in the range of low g values, and, now, in order to solve the problem, it is necessary to calculate the $f(g)$ correction function, which is, as yet, unknown. Equilibrium nucleus-size distribution $n(g)$ is derived from relation (3) by substituting the $\chi_g^{(v)}(T)$ function (8) and the $\chi_g^{(t)}$ and $\chi_g^{(r)}$ functions in explicit form (3a) into it:

$$n(g) = n_1 g^{\frac{3}{2}} \left(\frac{I_g^3}{I_{1x} I_{1y} I_{1z}} \right)^{\frac{1}{2}} \exp\left[\frac{(g-1)(\mu_1 - \mu_{liq}) - \alpha(g^{2/3} - 1) + P_\infty v(g-1) - f(g) + f(1)}{kT} \right] \cong n_1 \exp\left[(g-1)\left(\ln S_v + \frac{v}{V_\infty} \right) - \frac{\alpha(g^{2/3} - 1) + f(g) - f(1) - 4kT \ln g}{kT} \right], \quad (9)$$

where $S_v = \dfrac{P_1}{P_\infty(T)}$ is the vapor supersaturation and $V_\infty = \dfrac{1}{n_\infty(T)} = \dfrac{kT}{P_\infty(T)}$ is the volume per molecule in the saturated vapor. As $\dfrac{v}{V_\infty} \ll 1 \le \ln S_v$, this term will be omitted below. When Eq. (9) was derived, it was taken into account that liquid clusters have no symmetry axes, $\gamma_g = 1$; however, their shape is almost spherical and the moments of inertia are $I_g \cong I_1 g^{5/3}$ [5].

Note that relation (9) can be used to completely solve the problem concerning the determination of the equilibrium nucleus-size distribution for the macroscopic case ($g \to \infty$). Indeed, the pre-exponential factor is, here, determined, while the exponent is, after ignoring the correction function, a logarithmic term, unities as compared with g are equal to the classical formation work of a droplet, and we have the following:

$$n(g) = n_1 \exp\left[\frac{gkT \ln S_v - \alpha g^{2/3}}{kT} \right].$$

In the region of microscopic nuclei and the transition region, distribution (9) is somewhat similar to the result obtained in [20] and resembles the relation for the self-consistent correction to the classical theory (SCCCT) [21, 22] (the former classical theory with the Barnard correction [23]), but, in contrast to them, it comprises the as yet unknown correction function $f(g)$ and the term with ln$g$.

A simple molecular-kinetic analysis has shown that, because of the deficiency of neighbors, the energy of molecule binding on a droplet surface or in a cluster is lower than that for a molecule on a planar liquid surface and, the smaller an object, the lower the energy [5, 9]. For any vapor supersaturation, there is a critical size of a nucleus occurring at unstable equilibrium with a vapor; nuclei with smaller sizes occur in the medium of an unsaturated vapor and evaporate, while supercritical nuclei are in the medium of a supersaturated vapor and, therefore, grow. Nucleus-size distributions are known to have a minimum at a point corresponding to the critical size. Therefore, calculating logarithmic distribution (9), differentiating it with respect to g, and equating the derivative to zero, we find the minimum of the distribution, which determines number g^* of molecules in a critical nucleus:

$$\ln S_v = \frac{2\alpha}{3kTg^{*1/3}} + \frac{1}{kT} \left. \frac{\partial f(g)}{\partial g} \right|_{g^*} - \frac{4}{g^*}. \quad (10)$$

Expression (10) is valid for both macroscopic and microscopic nuclei. The comparison of Eq. (10) with the Thomson equation

$$\ln S_v = \frac{2\alpha}{3kTg^{*1/3}} \quad (11)$$

shows that the supersaturation of a vapor occurring at unstable equilibrium with a critical nucleus of size g^* somewhat differs from the supersaturation over a classical droplet with the same size in the existence of factors containing derivative $\frac{\partial f(g)}{\partial g}$ and Lothe–Pound correction $4/g^*$. Hence, both the flux of molecules condensing on the surface of a critical nucleus and the equal flux of evaporating molecules are changed. Therewith, the evaporation rate of a quiescent and nonrotating nucleus differs from the evaporation rate of an equisized classical droplet by $\exp\left(\frac{1}{kT}\frac{\partial f(g)}{\partial g}\Big|_{g^*}\right)$ times because of the small sizes. Let us use this fact for the determination of the $f(g)$ function.

It should also be noted that the same conclusions regarding different evaporation rates of a nucleus and an equisized classical droplet and on the fact that the true evaporation rate of clusters leads to solving the problem of nucleation also directly follow from analysis of the Becker and Döring work [2].

3. THE EFFECT OF FLUCTUATIONS ON DROPLET EVAPORATION RATE

Traditionally, the difference between small nucleus clusters and macroscopic droplets is related only to an increased role of the surface energy when describing their properties. This difference is, or course, important, but it is not the only one. It is known that the physical parameters of a macroscopic body occurring at equilibrium are, with a high accuracy, equal to their average values. Nevertheless, deviations from the average values do take place (indicating that the parameters fluctuate). The relative magnitude of the fluctuations increases with decreasing number of molecules in a body [18]. Therewith, the average physical values, the functions of thermodynamic parameters, are, already, noncoincident with their functions of averages, in contrast to the state of affairs that always holds in thermodynamics. Therefore, another essential difference between small and macroscopic bodies is the modification of their properties under the action of fluctuations. The probability distribution of small fluctuations obeys the Gauss law

$$w(x)dx = \frac{1}{\sqrt{2\pi\langle x^2\rangle}}\exp\left(\frac{-x^2}{\langle x^2\rangle}\right)dx, \qquad (12)$$

where $x = X - \langle X\rangle$ is the amplitude of fluctuations of any physical value X (the angle brackets denote averaging). Equation (12) may be used to calculate the average value of any physical parameter. In particular, the average squared temperature fluctuation $\langle(\Delta T)^2\rangle$ is equal to

$$\langle(\Delta T)^2\rangle = \frac{kT^2}{C_v}, \qquad (13)$$

here, $C_v = c_v g$ is the specific heat of a body at a constant volume, g is the number of molecules in the body, and c_v is the specific heat of a molecule. As can be seen from Eq. (13), the root-mean-square temperature fluctuation increases inversely to the square root of the number of particles upon decreasing body sizes.

In addition to the thermodynamic values, a body is characterized by the momentum of its macroscopic motion relative to a medium. In an equilibrium state, there is no motion and the momentum is equal to zero. However, the motion arises due to fluctuations. The average squared fluctuation for each of Cartesian components of velocity v_i is equal to $\langle v_i^2\rangle = \frac{kT}{mg}$; however, it is also inversely proportional to the number of molecules in the body. Velocity fluctuations are statistically independent of the fluctuations of other thermodynamic values, and, when body sizes decrease to values comparable with molecular sizes, continuous velocity fluctuations manifest themselves as the usual thermal motion. The same is valid for average squared angular velocities of body rotations, $\langle\omega_i^2\rangle = \frac{kT}{I_i(g)}$, with extrapolation of the average squared translational and angular velocities to molecular sizes (to $g = 1$), yielding values exactly equal to those obtained using the equipartition law of statistical physics. Thus, the fluctuations turn out to be an instrument that enables one to rather precisely predict the behavior of microphysical objects in terms of thermodynamics.

When considering the above nucleus clusters as macromolecules undergone translational and rotational motions, we, from the point of view of thermodynamics, have taken into account variations in the equilibrium distribution of clusters and in the size of a critical nucleus caused by fluctuations in their translational and angular velocities. However, fluctuations not only are responsible for the development of thermal motion but also affect the internal energy of a nucleus as a whole via time variations in its temperature and intermolecular interaction energy. In particular, we would like to determine fluctuation-induced variations in the evaporation rate of nuclei, as compared with the evaporation rate of equisized classical droplets, because this would enable us to find derivative $\frac{\partial f}{\partial g}\Big|_{g^*}$ from Eq. (10) and obtain correction function $f(g)$. Since, so far, no one knows how to calculate the properties of clusters, it is proposed, initially, to calculate the droplet-evaporation rate taking into account the corrections for the fluctuations (not only a droplet itself, but also any small deformation is considered to be macroscopic!) and, then, to determine the rate of cluster evaporation by extrapolating the obtained dependence to the region of nucleus sizes. It is supposed that the rate of cluster evaporation found in this way will be close to the true one, because the size

(radius) of critical nuclei is only a few times smaller than the radius of the smallest droplets to which thermodynamics is applicable.

The rate of the isothermal evaporation of a macroscopic spherical droplet $Q_0(g,T)$ is determined by the number of molecules leaving the droplet surface per unit time [18]:

$$Q_0(g) = a_{ac} n_\infty(T)\sqrt{\frac{kT}{2\pi m}} \times 4\pi r_0^2 g^{2/3} \exp\left(\frac{2\alpha}{3kTg^{1/3}}\right), \quad (14)$$

where a_{ac} is the accommodation coefficient. Because of fluctuations, the droplet temperature at each moment slightly differs from medium temperature T; the droplet is not quite spherical, and its shape and surface area ξ continuously somewhat vary. The droplet-evaporation rate also fluctuates following variations in its temperature, shape, and surface area. The effect of fluctuations in the temperature and shape of clusters on the rate of their evaporation was distinctly seen in molecular dynamic experiments [24].

If the probability distribution is known for fluctuations of droplet parameters, the evaporation rate may be found by averaging over this distribution, the determination of which is our immediate problem. Probability w that a droplet is in a state with $(T + \Delta T)$ and $(\xi + \Delta\xi)$ [18] is proportional to

$$w \sim e^{\Delta S_a} = e^{\frac{-R_{min}}{kT}}. \quad (15)$$

Here $\Delta S_a = -R_{min}/kT$ is the fluctuation-related change in the total entropy of a closed system and $R_{min} = \Delta E - T\Delta S + P\Delta V$ is the minimum work required for the preset reversible change in the droplet parameters, where ΔE, ΔS, and ΔV are the changes in the energy, entropy, and volume of the droplet, respectively. Further, let us, in the minimum work, omit term $P\Delta V$, which describes the work of a medium for fluctuation changes in the droplet volume, thereby supposing that the system temperature is far from the critical one, and, therefore, the liquid compressibility may be ignored and the droplet volume may be considered to be constant, $\Delta V = 0$. Expression (15) is valid for both large and small fluctuations. Since we are interested only in the most probable small fluctuations, we expand ΔE into a series to the second-order terms (inclusive) to find R_{min} in the following form:

$$R_{min} = \sigma\Delta\xi + \frac{1}{2}\left[\frac{\partial^2 E}{\partial S^2}(\Delta S)^2 + 2\frac{\partial^2 E}{\partial S\partial\xi}\Delta S\Delta\xi + \frac{\partial^2 E}{\partial\xi^2}(\Delta\xi)^2\right].$$

The bracketed expression may be represented as the following sum of the products of differentials:

$$\frac{1}{2}\left[\Delta S\Delta\left(\frac{\partial E}{\partial S}\right)_\xi + \Delta\xi\Delta\left(\frac{\partial E}{\partial\xi}\right)_S\right] = \frac{1}{2}(\Delta S\Delta T + \Delta\sigma\Delta\xi).$$

Thus, we obtain the probability of fluctuation (15) as follows:

$$w \sim \exp\left(-\frac{\sigma\Delta\xi}{kT} - \frac{\Delta S\Delta T + \Delta\sigma\Delta\xi}{2kT}\right). \quad (16)$$

Expressing ΔS and $\Delta\sigma$ via variables T and ξ, we derive

$$\Delta S = \frac{C_v}{kT}\Delta T - \frac{d\sigma}{dT}\Delta\xi, \quad \Delta\sigma = \frac{d\sigma}{dT}\Delta T,$$

and, substituting these expressions into relation (16), we arrive at

$$w \sim \exp\left(-\frac{\sigma\Delta\xi}{kT} - \frac{C_v}{2kT^2}(\Delta T)^2\right). \quad (17)$$

The obtained probability distribution desintegrates into two factors, which depend only on ΔT or only $\Delta\xi$. Hence, the shape and temperature fluctuations are statistically independent; i.e., $\langle\Delta T\Delta\xi\rangle = 0$. This enables us to take into account these fluctuations separately.

Let us begin with the shape fluctuations of an incompressible liquid droplet containing a preset number of molecules. The surface area per se provides no information on the droplet shape, because many droplets with different shapes correspond to the same surface area. Small droplet shape fluctuations manifest themselves as diverse convexities, indentations, flattenings, etc., with different sizes and shapes arising and disappearing on a spherical surface. According to relation (17), configurations with a minimum increment of the surface area, as compared with the initial spherical droplet, are most probable, and these configurations must primarily be taken into account.

If small volume ΔV is subtracted from a spherical droplet composed of g molecules, the residual droplet volume and this small volume form new spherical droplets under the action of surface tension. In this situation, their surface areas will be minimum. If complete separation has not been reached and the body of the droplet and small volume ΔV have a common base, surface tensions will compress them into ball segments constructed on the common circular base. The surface area of this construction will, obviously, be minimum for the preset deformation volume ΔV and the base area. If the droplet surface contains a dent with volume ΔV, it may be concluded that the configuration consisting of the ball segments of the droplet body and the dent will have the minimum surface area for preset volume ΔV and the base area. Deformed droplets with any other segment shapes other than spherical are characterized by larger surface area increments; therefore, the probability of their formation is negligibly low because of the strong exponential $w(\Delta\xi)$ dependence of the probability on the increment (17). So, we may ignore the contribution of all other droplet configura-

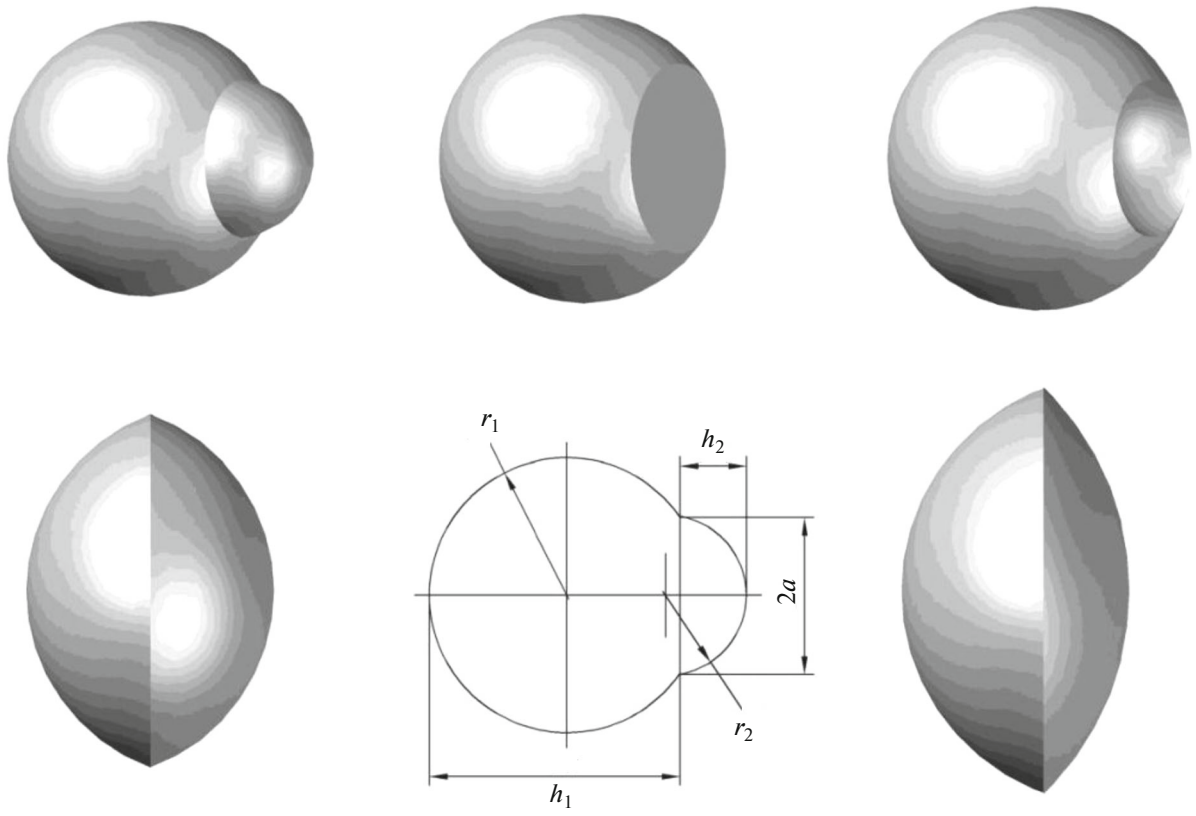

Fig. 1. Schematic representation of deformed droplets.

tions to the evaporation process and consider only the most probable deformed droplets composed of two ball segments. This approach simplifies the calculations, while making it possible to take into account the effect of droplet-shape fluctuations on the rate of droplet evaporation.

Imagine that, as a result of fluctuations, a spherical droplet with radius $r = r_0 g$ acquires the shape of a figure consisting of two ball segments. The first segment with a larger volume (mass) and curvature radius r_1, which slightly differs from r, is bonded to the second ball segment in the form of a convexity or a dent with radius r_2 via a common base with radius a (Fig. 1). Surface area ξ of this deformed droplet composed of g molecules is equal to [25]

$$\begin{aligned}\xi(r_1, r_2, a) &= 2\pi r_1 h_1 + 2\pi r_2 h_2 \\ &= 2\pi[r_1(r_1 + \sqrt{r_1^2 - a^2}) + r_2(r_2 - \sqrt{r_2^2 - a^2})],\end{aligned} \tag{18}$$

where $h_{1,2} = r_{1,2} \pm \sqrt{r_{1,2}^2 - a^2}$ denotes the heights of the segments. The incompressibility of the liquid makes it possible to express r_2 via r_1 and a as follows:

$$\begin{aligned}\frac{4}{3}\pi r^3 &= \frac{\pi}{3}h_1^2(3r_1 - h_1) \pm \frac{\pi}{3}h_2^2(3r_2 - h_2) \\ &= \frac{\pi}{3}[(r_1 + \sqrt{r_1^2 - a^2})^2(2r_1 - \sqrt{r_1^2 - a^2}) \\ &\pm (r_2 - \sqrt{r_2^2 - a^2})(2r_2 + \sqrt{r_2^2 - a^2})].\end{aligned} \tag{19}$$

Here and below, the signs "+" and "−" correspond to droplets deformed via the formation of a convexity or a dent, respectively. Introducing denotations $\rho_1 = r_1/r = r_1/r_0 g^{1/3}$, $\rho_2 = r_2/r_0 g^{1/3}$, $\lambda = a/r_0 g^{1/3}$, and $\eta = \xi/4\pi r^2 = \xi/4\pi r_0^2 g^{2/3}$, Eqs. (18) and (19) may be written, respectively, as follows:

$$\begin{aligned}\eta(\rho_1, \rho_2, \lambda) = \frac{1}{2}\Big[&\rho_1\left(\rho_1 + \sqrt{\rho_1^2 - \lambda^2}\right) \\ &+ \rho_2\left(\rho_2 - \sqrt{\rho_2^2 - \lambda^2}\right)\Big],\end{aligned} \tag{20}$$

$$\begin{aligned}4 &= (\rho_1 + \sqrt{\rho_1^2 - \lambda^2})^2(2\rho_1 - \sqrt{\rho_1^2 - \lambda^2}) \\ &\pm (\rho_2 - \sqrt{\rho_2^2 - \lambda^2})^2(2\rho_2 + \sqrt{\rho_2^2 - \lambda^2}).\end{aligned} \tag{21}$$

Equations (20) and (21) were solved numerically, and ρ_2 and η were found as functions of their variables ρ_1 and λ. Analysis of the solution shows that, for any value of ρ_1, the surface area of the deformed droplet

rapidly increases, while the probability of the deformed droplet formation drastically decreases with a reduction in base radius λ from 1 to 0. An important consequence of this phenomenon is the fact that the probability of the formation of a deformed droplet that has two or more convexities or dents or convexities and dents simultaneously is negligibly low, with the exception of the range of $0.9 < \lambda \le 1$, which, however, does not noticeably contribute to the correction to the evaporation rate of a droplet subjected to fluctuations.

According to relation (17), the probability of finding a deformed droplet with reduced radii of the large segment and base equal to ρ_1 and λ, respectively, may be written in the following form:

$$w(g,\rho_1,\lambda)d\rho_1 d\lambda = A(g)\exp\left(-\frac{\alpha g^{2/3}(\eta(g,\rho_1,\lambda)-1)}{kT}\right)d\rho_1 d\lambda, \quad (22)$$

where $A(g)$ is determined from the following normalization condition:

$$A(g)\iint\limits_{\rho_1,\lambda}\exp\left[-\frac{\alpha g^{2/3}(\eta(g,\rho_1,\lambda)-1)}{kT}\right]d\rho_1 d\lambda = 1. \quad (23)$$

The integration is, here, carried out over all possible ρ_1 and λ values. Using Eq. (14), the evaporation rate of a deformed droplet may be represented as follows:

$$\begin{aligned} Q(g,\rho_1,\lambda) = Q_0(g)\Bigg\{&\frac{1}{2}\rho_1\left(\rho_1+\sqrt{\rho_1^2-\lambda^2}\right)\\ &\times\exp\left[\frac{2\alpha}{3g^{1/3}kT}\left(\frac{1}{\rho_1}-1\right)\right]\\ &+\left[\eta(g,\rho_1,\lambda)-\frac{1}{2}\rho_1\left(\rho_1+\sqrt{\rho_1^2-\lambda^2}\right)\right]\\ &\times\exp\left[\frac{2\alpha}{3g^{1/3}kT}\left(\frac{1}{\rho_2}-1\right)\right]\Bigg\}. \end{aligned} \quad (24)$$

Averaging $Q(g, \rho_1, \lambda)$ over distribution (22), we obtain the following equation for evaporation rate $Q_c(g)$ of a droplet subjected to shape fluctuations:

$$\begin{aligned} Q_c(g) &= \langle Q(g)\rangle = A(g)\\ &\times\iint\limits_{\rho_1,\lambda} Q(g,\rho_1,\lambda)\exp\left[-\frac{\alpha g^{2/3}(\eta(g,\rho_1,\lambda)-1)}{kT}\right]d\rho_1 d\lambda\\ &= Q_0(g)\varphi(g), \end{aligned} \quad (25)$$

where $\varphi(g) = Q_c(g)/Q_0(g)$ is the evaporation rate ratio between a droplet consisting of g molecules and subjected to shape fluctuations and an identical "classical" droplet. It can be easily seen from relations (23)–(25) that $\varphi(g)$ depends on the sole dimensionless parameter, which characterizes the substance of a droplet, namely, $\alpha/kT = 3\sigma v/r_0 kT$. The $\varphi(g, \alpha/kT)$ value was numerically calculated by relations (22)–(25) for droplets composed of 4, 6, 8, 15, 27, 64, 125, 250, and 512 molecules and α/kT values from 7 to 36; the $\varphi(g, \alpha/kT)$ values refined as compared with those presented in [16] are listed in Table 1.

As follows from Table 1, shape fluctuations noticeably affect the evaporation rate of clusters containing up to 512 molecules. The highest evaporation rates are reached at high α/kT values, i.e., for high-molecular-mass substances possessing a high surface tension at decreased temperatures.

Now, let us consider the effect of temperature fluctuations on the evaporation rate of droplets. The distribution of temperature fluctuations has a Gaussian form, with its normalization constant being calculated analytically and finally written in the form of Eq. (12). The evaporation rate of a droplet subjected to fluctuations of its shape and temperature may be found by simple averaging of the obtained rate $Q_c = \varphi Q_0$ over distribution (12) with $\langle(\Delta T)^2\rangle$ from (13). However, a more intelligent method consists in the Taylor expansion of droplet evaporation rate $Q_c = \varphi Q_0(T)$ in terms of ΔT to the second-order terms (inclusive) [26],

$$\begin{aligned} Q_c(T+\Delta T) &= \varphi Q_0(T+\Delta T) = \varphi(T)Q_0(T)\\ &+\varphi(T)\left.\frac{dQ_0}{dT}\right|_T\Delta T+\frac{1}{2}\varphi(T)\left.\frac{d^2Q_0}{dT^2}\right|_T(\Delta T)^2, \end{aligned} \quad (26)$$

followed by averaging. In the latter expression, we have ignored the temperature dependence of φ as compared with exponential $Q_0(T)$ dependence (14); it can be easily shown that allowance for the former dependence does not lead to significant changes in $Q_c(T+\Delta T)$. By averaging the latter expression and taking into account that $\langle\Delta T\rangle = 0$, we find evaporation rate $Q_f(g,T)$ of a droplet subjected to fluctuations of its shape and temperature as follows:

$$\begin{aligned} Q_f(g,T) &= \langle\varphi Q_0(T+\Delta T)\rangle = \varphi(g,T)Q_0(g,T)\\ &+\frac{1}{2}\varphi(g,T)\left.\frac{d^2Q_0}{dT^2}\right|_T\langle(\Delta T)^2\rangle. \end{aligned} \quad (27)$$

Substituting $\langle(\Delta T)^2\rangle$ from Eq. (13) into Eq. (27) and calculating the second derivative, we have

$$\begin{aligned} Q_f(g,T) &= \varphi(g,T)Q_0(g,T)\\ &\times\Bigg\{1+\frac{q}{2cTg}\left(\frac{q}{kT}-3\right)+\frac{1}{2g}\left(\frac{3k}{4c}+\frac{c_p}{c}-1\right)\\ &-\frac{4\pi r_0^2}{cTg^{4/3}}\left(\sigma-T\frac{d\sigma}{dT}\right)\left(\frac{2q}{3kT}-1\right)\\ &+\frac{32\pi^2 r_0^4}{9ckT^2g^{5/3}}\left(\sigma-T\frac{d\sigma}{dT}\right)\Bigg\} = \varphi(g,T)\psi(g,T)Q_0(g,T). \end{aligned} \quad (28)$$

The analysis of Eq. (28) shows that the evaporation rate of a quiescent and nonrotating cluster with fluctuating shape and temperature is higher than that of a classical droplet with the same size, because $\varphi \ge 1$ and

Table 1. Calculated values of the $\varphi(g, \alpha/kT)$ function

α/kT	g									
	2	4	6	8	15	27	64	125	250	512
	$\varphi(g, \alpha/kT)$									
7	1.0	0.883	1.012	1.050	1.058	1.042	1.022	1.012	1.007	1.004
8	1.0	0.898	1.030	1.067	1.069	1.049	1.024	1.014	1.007	1.004
9	1.0	0.910	1.050	1.086	1.081	1.056	1.027	1.015	1.008	1.005
10	1.0	0.925	1.072	1.105	1.093	1.063	1.030	1.016	1.009	1.005
11	1.0	0.943	1.094	1.125	1.107	1.071	1.033	1.018	1.010	1.006
12	1.0	0.962	1.118	1.146	1.122	1.080	1.037	1.020	1.011	1.006
13	1.0	0.982	1.143	1.168	1.137	1.090	1.041	1.022	1.012	1.007
14	1.0	1.004	1.169	1.191	1.155	1.101	1.046	1.025	1.013	1.008
15	1.0	1.027	1.196	1.216	1.174	1.113	1.052	1.028	1.015	1.008
16	1.0	1.052	1.224	1.249	1.195	1.126	1.058	1.031	1.017	1.009
17	1.0	1.077	1.253	1.270	1.219	1.142	1.065	1.035	1.019	1.010
18	1.0	1.104	1.284	1.299	1.244	1.159	1.073	1.040	1.022	1.011
19	1.0	1.132	1.316	1.331	1.273	1.178	1.083	1.046	1.025	1.013
20	1.0	1.161	1.350	1.365	1.306	1.200	1.094	1.052	1.029	1.015
21	1.0	1.191	1.386	1.401	1.342	1.225	1.108	1.060	1.034	1.017
22	1.0	1.223	1.424	1.440	1.382	1.253	1.124	1.070	1.041	1.020
23	1.0	1.255	1.465	1.483	1.428	1.286	1.142	1.083	1.049	1.023
24	1.0	1.290	1.507	1.529	1.479	1.324	1.165	1.098	1.059	1.028
25	1.0	1.325	1.553	1.58	1.538	1.368	1.192	1.116	1.072	1.034
26	1.0	1.363	1.601	1.634	1.605	1.419	1.225	1.139	1.088	1.041
27	1.0	1.402	1.653	1.694	1.681	1.479	1.265	1.168	1.110	1.051
28	1.0	1.442	1.708	1.759	1.767	1.549	1.314	1.204	1.138	1.064
29	1.0	1.485	1.768	1.831	1.866	1.631	1.373	1.249	1.174	1.081
30	1.0	1.530	1.831	1.910	1.980	1.727	1.446	1.306	1.221	1.103
31	1.0	1.577	1.890	1.996	2.111	1.840	1.535	1.379	1.283	1.132
32	1.0	1.626	1.973	2.092	2.261	1.974	1.645	1.470	1.363	1.171
33	1.0	1.677	2.052	2.197	2.435	2.132	1.780	1.586	1.468	1.222
34	1.0	1.737	2.137	2.313	2.635	2.319	1.948	1.733	1.606	1.291
35	1.0	1.788	2.228	2.442	2.866	2.542	2.155	1.921	1.786	1.382
36	1.0	1.848	2.328	2.585	3.134	2.806	2.413	2.159	2.023	1.502

$\psi \geq 1$. A noticeably higher evaporation rate than that of the classical one ($Q_f(g,T) \approx 10Q_0(g,T)$) is reached only for small clusters consisting of 5–15 molecules and at relatively low temperatures. As the droplet size and temperature are increased, the evaporation rate of a cluster subjected to fluctuations approaches the evaporation rate of a classical droplet because of a rapid decrease in $\varphi(g)$ and a slower reduction in $\psi(g)$ to unity.

4. FORMATION RATE OF MICROSCOPIC NUCLEI. COMPARISON OF PROPOSED THEORY WITH EXPERIMENTAL DATA AND PREDICTIONS OF THE CLASSICAL NUCLEATION THEORY

In the previous section, we have determined the difference between the evaporation rates of quiescent and nonrotating clusters composed of g molecules and the evaporation rate of classical droplets consisting of

the same number of molecules, with this difference being due to the small sizes of the objects, thereby finding derivative $\frac{\partial f}{\partial g}$ of the correction function entering into Eq. (10):

$$\frac{\partial f}{\partial g} = kT \ln[\varphi(g,T)\psi(g,T)]. \quad (29)$$

Correction coefficients $\varphi(g)$ and $\psi(g)$ have been calculated in terms of the fluctuation theory for macroscopic droplets and extrapolated to the region of small sizes (no more than 100 molecules in a cluster). Relation (29) is strict for macroscopic droplets (composed of 1000 or more molecules); its accuracy for nucleus microscopic clusters is to be additionally verified by comparison with reliable experimental data.

Equation (10), which relates the critical nucleus size to vapor supersaturation, is, now, written in the following form:

$$\ln S_v = \frac{2\alpha}{3kTg^{*1/3}} + \ln\varphi(g^*,T) + \ln\psi(g^*,T) - \frac{4}{g^*}. \quad (30)$$

As follows from Eq. (30), at low temperatures, the size of a critical nucleus is noticeably larger than that of a classical droplet predicted by Thomson equation (11); however, the nucleus size may be even somewhat smaller than the classical one because of the Lothe–Pound correction ($-4/g^*$) at high temperatures, when $\varphi \cong 1$ and $\psi \cong 1$.

Integrating Eq. (29) over g at T = const and substituting the obtained $f(g)$ function into relation (9), we arrive at the following final expression for the equilibrium size distribution of nucleus clusters:

$$n(g) = n_1 g^4 \exp\left\{(g-1)\ln S - \frac{\alpha(g^{2/3}-1)}{kT} - \int_1^g \ln[\psi(g)]\,dg - \int_2^g \ln[\varphi(g)]dg\right\}. \quad (31)$$

Since variations in the shape at a constant volume are possible only for clusters consisting of three and more molecules, the lower limit was taken to be two when integrating $\ln[\varphi(g)]$ in Eq. (31). At a known nucleus size distribution, the rate of nucleation has the following form [3, 15]:

$$J(g^*(S),T) = n(g^*)Z(g^*)\beta(g^*) = n(g^*)Z(g^*)2a_{ac}P_1\sqrt{\frac{2(g^*+1)\pi}{mg^*kT}}r_0^2\left(g^{*\frac{1}{3}}+1\right)^2, \quad (32)$$

where $Z(g^*) = \sqrt{\frac{1}{2\pi}\left(\frac{\partial^2 \ln n(g)}{\partial g^2}\right)_{g=g^*}}$ is the Zel'dovich factor and $\beta(g^*)$ is the rate of vapor molecule attachment to a critical nucleus. Here, in contrast to the CNT, it has been taken into account in $\beta(g^*)$ that vapor molecules are condensed on nuclei subjected to thermal motion.

Having selected a $\varphi(g)$ function suitable for approximating the data presented in Table 1 (see Appendix) and using relations (30)–(32) with the $\psi(g)$ function determined by expression (28), we may easily calculate nucleation rate J [$cm^{-3}\,s^{-1}$] and supersaturation S_v of a vapor occurring at equilibrium with clusters of the critical size at preset temperature T and compare them with experimental data. For these calculations, it is necessary to know the parameters of a studied liquid, such as surface tension $\sigma(T)$, saturation vapor pressure $P_\infty(T)$, liquid density $\rho(T)$, latent heat of evaporation $q(T)$, liquid specific heat c, and the approximate c_p/c ratio between vapor specific heat c_p at a constant pressure and the specific heat of the liquid.

Well-studied water, as well as dibutyl phthalate (DBP) and *n*-propanol, were used as the objects for comparing the proposed theory with experimental data on nucleation. Water nucleation at temperatures below 0°C is being intensely studied because of its role in atmospheric processes. DBP and alcohols, in particular, propanol, have appeared convenient objects for investigating nucleation in a so-called "laminar flow diffusion chamber," where supersaturation is created in a cooling laminar flow of a carrier gas preliminarily saturated with the vapor of a studied substance. The physicochemical parameters presented in Table 2 were used in the calculations. Latent heats of evaporation q were determined from the known temperature dependences of saturation vapor pressure:

$$\frac{d\ln P_\infty}{d\left(\frac{1}{T}\right)} = -\frac{q}{k},$$

while masses of molecules and specific heats were taken from handbook [27].

4.1. Water

Figure 2 illustrates the results of measuring the rate of water nucleation in a Wilson chamber performed by Viisanen et al. [30] in comparison with the data of calculations by expressions (31) and (32) proposed in this work and the predictions of the CNT for temperatures of 259, 253.7, 248.5, 244.1, and 238.8 K. It can be seen that the results of this work coincide with the measured nucleation rates within the experiment error, while the nucleation rates predicted by the CNT are, in all cases, nearly two decimal orders of magnitude higher than the measured ones. Unfortunately, we failed to calculate the nucleation rates and compare the theory with experimental data obtained at lower temperatures because of the abnormal behavior of supercooled water. At temperatures below 250 K, its density rapidly decreases and its specific heat rapidly

Table 2. Physicochemical properties of the used substances: mole mass M [g/mol], saturation vapor pressure P_∞ [dyne/cm^2], liquid density ρ [g/cm^3], surface tension σ [dyne/cm], liquid specific heat c [erg/(mol K)], and ratio between specific heats of a vapor at a constant pressure and a liquid c_p/c

Substance and its characteristics	Reference
Supercooled water	
$M = 18.02$	[27]
$\ln P_\infty(T) = 26 - 4050/T - 184000/T^2$	[27]
$\rho(T) = 1.004 - 0.22/(T - 230)$	[28]
$\sigma(T) = 93.6635 + 0.009133T - 0.275 \times 10^{-3}T^2$	[14, 35]
$c(T) = 1.8 \times 10^8[4.06 + 475/(T - 217)^2]$	[29]
$c_p/c = 0.45$	[27]
Dibutyl phthalate	
$M = 278.35$	[27]
$\log P_\infty(T) = 10.1899 - 1666/T - 547700/T^2$	[33]
$\sigma(T) = 33.93 - 0.0894(T - 293.15)$	[33]
$\rho(T) = 1.0492 - 0.67 \times 10^{-3}(T - 293.15)$	[33]
$c(T) = 4.577 \times 10^9 + 7.528 \times 10^6(T - 273.15)$	[34]
$c_p/c = 0.8$	[27]
n-Propanol	
$M = 60.09$	[27]
$\ln P_\infty(T) = 84.6957 - 8559.6064/T - 9.29\ln T + \ln 1333.22$	[14]
$\rho(T) = 0.82 - 0.818 \times 10^{-3}(T - 273.15) + 1.08 \times 10^{-6}(T - 273.15) - 16.5 \times 10^{-9}(T - 273.15)^3$	[14]
$\sigma(T) = 25.28 - 0.0839(T - 273.15)$	[14]
$c(T) = 2.518 \times 10^9[0.526 + 0.0024(T - 273.15)]$	[27]
$c_p/c = 0.59$	[27]

increases with decreasing temperature [31]. It is assumed that, in a range of 225–230 K, the specific heat passes through a maximum, while the density of supercooled water dramatically decreases. Because of the strong uncertainty in the values of the specific heat and density at low temperatures, the comparison between the predictions of the theory and the experimental data was limited from below by the region suitable for the direct measurements of these parameters, namely, by temperature values above 236 K.

4.2. Dibutyl Phthalate

Now, let us consider DBP. Figure 3 shows the dependences measured in [32, 33] for supersaturation S_v of DBP vapor occurring at equilibrium with critical nuclei composed of g^* molecules in comparison with the data calculated by relation (3) and Thomson equation (11) at nucleation temperatures of 249.65, 259.65, 269.15, and 279.65 K. It can be seen that the logarithmic values of supersaturation calculated for DBP vapor by Eq. (30) agree with the measured data within the experiment error for a temperature range of 249.65–269.15 K; at 279.65 K the calculation underestimates the experimental values by 5%. At the same time, the Thomson equation predicts logarithmic values of the supersaturation 12–15% lower than the experimental data. Accordingly, the numbers of molecules in critical nuclei calculated by Eq. (30) for these temperatures turn out to be 1.35–1.5 times larger than those in classical "Thomson" nuclei.

Comparison between the predictions of the proposed theory and the nucleation rates measured by Hämeri and Kulmala for DBP vapors in a laminar flow diffusion chamber [36] has shown (Fig. 4) that, at temperatures higher than 300 K, the calculated nucleation rates (solid lines) coincide with the experimental data (symbols). At 296.9 K, the calculation overestimates the nucleation rates by two to three times. Quantitative agreement between the CNT (dashed lines) and experimental data is absent. Below room temperature, the differences between the predictions of this work and the measurement results [36] increase with decreasing temperature. The contemporary relation between the theoretical and experimental data on the nucleation of supersaturated DBP vapor is illustrated in Fig. 5, where the dependences of critical supersaturation on nucleation temperature are pre-

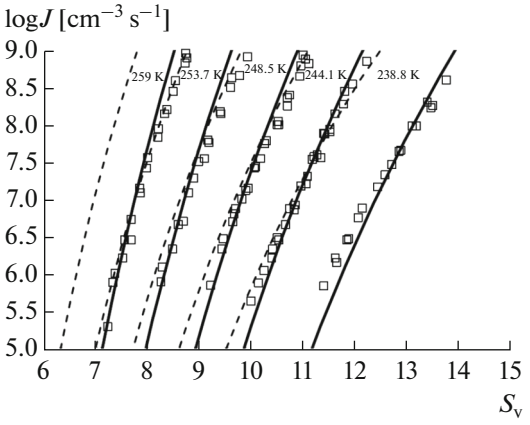

Fig. 2. Dependences of water-vapor nucleation rate J on supersaturation S_v measured in [30] (symbols) in comparison with data calculated by Eqs. (31) and (32) of this work (solid lines) and in terms of the CNT (dashed lines) for temperatures of 259, 253.7, 248.5, 244.1 and 238.8 K.

sented. Here, supersaturation, at which the nucleation rate is equal to 10^6 cm^{-3} s^{-1}, is considered to be critical. The critical supersaturation values measured in [32, 33] and by Hämeri and Kulmala [36] and Mikheev et al. [37] are shown in Fig. 5 as compared with the predictions of the theory that we propose, CNT, SCCCT [21, 22], and Dillmann–Meier theory [14].

It can be seen that the experimental data markedly differ from each other. In the vicinity of room temperature, the data of [36, 37] are almost the same; however, as the temperature decreases, the critical supersaturation values measured by Hämeri and Kulmala [36] are several times higher than the values obtained in, e.g., [33]. At $T = 250$ K, the critical supersaturation values and nucleation rates differ by 3 times and 3.5 orders of magnitude, respectively. The reasons for the discrepancies are obviously experiment errors and the use of not quite correct reference data. The main drawback of the experiments carried out by Vaganov et al. [33] was associated with the incorrect measurement of aerosol concentration, which resulted in the systematic underestimation of the nucleation rate by more than two orders of magnitude. In subsequent works [36, 37], this drawback was eliminated; however, they had other errors. In [36], they are (1) the use of an incorrect equation for the saturation pressure of DBP vapor and (2) ignorance of the effect of obtained aerosol evaporation during its delivery into the measurement volume of a particle counter. Let us consider these problems in greater detail.

(1) According to [38], an incorrect Antoine equation was used in [36] to calculate saturation vapor pressure P_∞ of DBP (in mm Hg),

$$\ln P_\infty = \left(16.27 - \frac{5099}{T - 109.65}\right), \qquad (33)$$

which is an approximation of the expression presented in Table 2 of this work and had been applied in [32, 33]. According to [39], the constant in the denominator of Eq. (33) is equal to $(0.19T_b - 18)$ K, where T_b is the boiling temperature of a substance at the normal pressure. For DBP, this constant is 98.47 K (rather than 109.65 K!). With this constant, the Antoine equation adequately reproduces the initial expression in Table 2: the predicted vapor pressure at $T = 246$ K differs from that calculated by the equation from Table 2 by no more than 10%. The critical supersaturation values, which were reported in [36], recalculated by the initial expression presented in Table 2 are denoted in Fig. 6 by rhombs. It can be seen that the critical supersaturation values reported in [36, 37] coincide after the recalculation; futhermore, these supersaturation values at temperatures higher than 290 K in a rather good agreement with the results of the proposed theory.

(2) It was noted in [33] that the study of nucleation at low temperatures was limited by the evaporation of an ultradispersed DBP aerosol during its transport to the region of enlargement and registration at temperatures close to the room temperature. In particular, the majority of an aerosol obtained at 249.65 K was evaporated when the transport time was ≥0.7 s, i.e., about 95% of particles with an average radius of about 3 nm disappeared within 0.7 s upon heating by 40–45 K. In [33, 36, 37], the experimental conditions were similar and the sizes of the obtained particles were almost equal. Therefore, the authors of the aforementioned works could not avoid the evaporation induced loss of a substantial part of an aerosol formed at decreased temperatures. The problem relevant to the evaporation of an aerosol formed at low temperatures and transported to the region of registration must be in the focus of researchers' attention. The matter is that a formed condensation aerosol is rather polydisperse. In the opinion of Fuks and Sutugin [40], the particle size distribution is most adequately described by the lognormal law. At a slight heating of an aerosol containing flow by 10–30 K, a relatively small number of the smallest particles are lost. Upon heating by 40–100 K, the majority of the aerosol is lost, and a fraction of 0.1, 0.01, etc., of the aerosol is registered. Aerosol evaporation is difficult to notice in an experiment, because some amount, albeit small, of a nonevaporated aerosol always enters the counter.

Mikheev et al. [37] discussed a possible loss of aerosol particles due to evaporation and presented the layout of a TSI Model 3025A counter, which was used in the work. The layout enables one to conclude that the counter plays the decisive role in aerosol evaporation. Indeed, the layout shows that the aerosol containing flow entering the counter is divided in a ratio of 1 : 10 and the minor flow is directed to the registration through the evaporator of the enlarging unit of the counter, with the evaporator being heated 40–50 K higher than the room temperature. The heating of the flow to only 30 K higher than room temperature

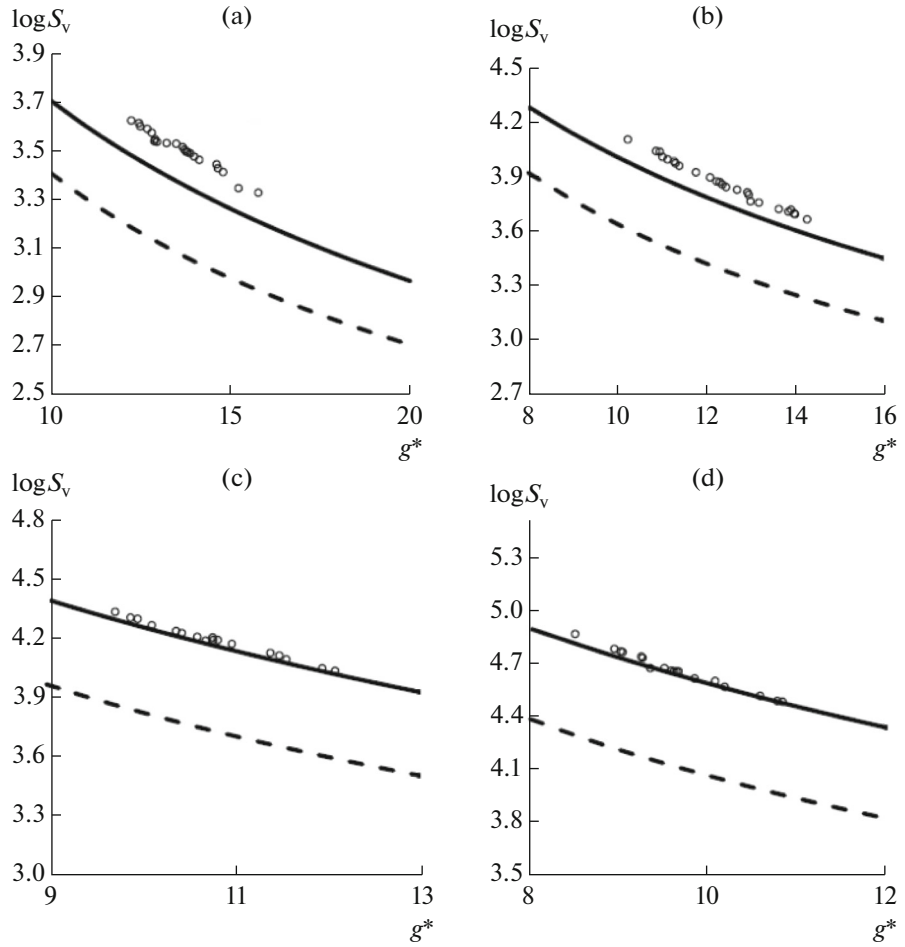

Fig. 3. Supersaturation S_v of DBP vapor occurring at equilibrium with critical nuclei composed of g molecules at temperatures of (a) 279.65, (b) 269.15, (c) 259.65, and (d) 249.65 K. Symbols denote experimental data of [32, 33], solid lines refer to results calculated by Eq. (30) of this work, and dashed lines reflect data calculated by Thomson equation (11).

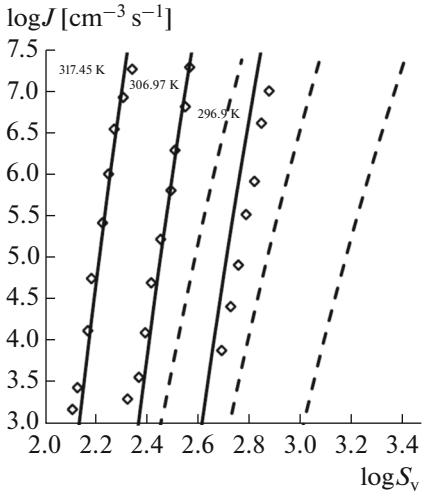

Fig. 4. Comparison between dependences of DBP vapor nucleation rates on supersaturation measured in [36] (symbols) and calculated by Eqs. (31) and (32) of this work (solid lines) and in terms of the CNT (dashed lines) at temperatures of 317.45, 306.97, and 296.9 K.

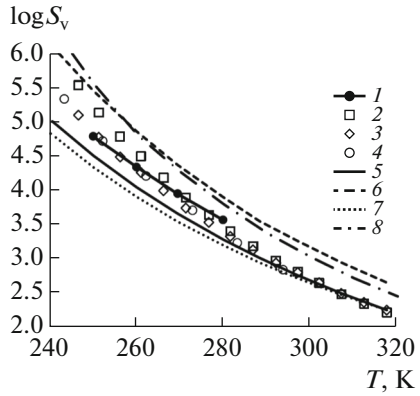

Fig. 5. Temperature dependences of critical supersaturation of DBP vapor ($J = 10^6$ cm^{-3} s^{-1}): (*1*) data from [33], (*2*) data from [36], (*3*) recalculation of data from [36], and (*4*) data from [37] compared with results of this work (solid line *5*) and predictions of the CNT (dashed line *6*), SCCCT (dots *7*), and Dillmann–Meier theory (dash-and-dot line *8*).

increases the DBP evaporation rate by ≈50 times. If such or higher heating (30 + 43 = 73 K) lasts at least 0.014 s or longer, the fraction of the evaporated aerosol will a fortiori be larger than that disappearing over 0.7 s at the room temperature. It should, in particular, be noted that the partial aerosol evaporation in the particle counter may explain the decrease in the DBP nucleation rate measured at 296.9 K as compared with the predictions of the proposed theory (see Fig. 4).

It is obvious that evaporation of aerosol particles leads to overestimating the critical supersaturation values measured in [36, 37] at temperatures below 290 K (see Fig. 5). The elimination of the effect of evaporation will make the temperature behavior of the critical supersaturation observed in these studies similar to that in [32, 33], thereby undoubtedly improving the agreement between experimental data and the proposed theory at low temperatures.

4.3. n-Propanol

Figure 6 illustrates experimental data obtained by Görke et al. [41] on the isothermal nucleation of supersaturated *n*-propanol vapor in helium, with these data being obtained in a laminar flow diffusion chamber at temperatures of 270, 280, 290, and 300 K, in comparison with the predictions of the theory proposed in this work and the CNT. For each temperature, the measurements were performed at different pressures of the carrier gas (helium): 50–60, 100, and 200 kPa. As can be seen in the figure, the experimental nucleation rates and those calculated in terms of the proposed theory at 270 K lie below the data predicted by the CNT; in the range between 280 and 290 K, they cross over the results of the CNT; and, at 300 K, they appear to lie higher than those predicted by the CNT. As for the quantitative state of affairs, the results obtained in terms of the proposed theory at 270 K coincide with the measured data at a carrier gas pressure of 200 kPa and exceed them by one to two orders of magnitude at pressures of 50 and 100 kPa. At temperatures of 280 and 290 K, the measured and calculated nucleation rates coincide with each other within the experiment error. At 300 K, the calculation yields rates underestimated approximately ten times.

A similar state of affairs, namely, a discrepancy between the measured nucleation velocities and the predictions of the proposed theory by as many as ten times, was also observed for ibuprofen [17].

The reasons for the quantitative discrepancies are anybody's guess. They may be explained by, on the one hand, the inaccuracy of the proposed theory and, on the other hand, any systematic errors in experiments.

CONCLUSIONS

Analysis of equilibrium nucleus-size distribution found in supersaturated vapor by the methods of statistical physics has shown that clusters consisting of 1000 or less numbers of molecules are microscopic objects. They are characterized by partition functions and cannot be described by thermodynamic methods. An approach has been proposed, which enables one to directly determine the partition function over the internal degrees of freedom of a cluster and express the nucleus size distribution via habitual temperature and supersaturation. It has been shown that, to find the partition function and the equilibrium nucleus size distribution, it is necessary to know the evaporation rate of the clusters. This rate has been approximately determined by extrapolating the refined evaporation rate obtained in terms of the fluctuation theory for incompressible liquid droplets to the region of nucleus sizes. As a result, a homogeneous stationary nucleation theory was formulated without the use of adjustable parameters. The theory employs ordinary thermodynamic values the same as those used in the CNT, as well as the specific heats of a studied liquid and its vapor at a constant pressure. The results of this work

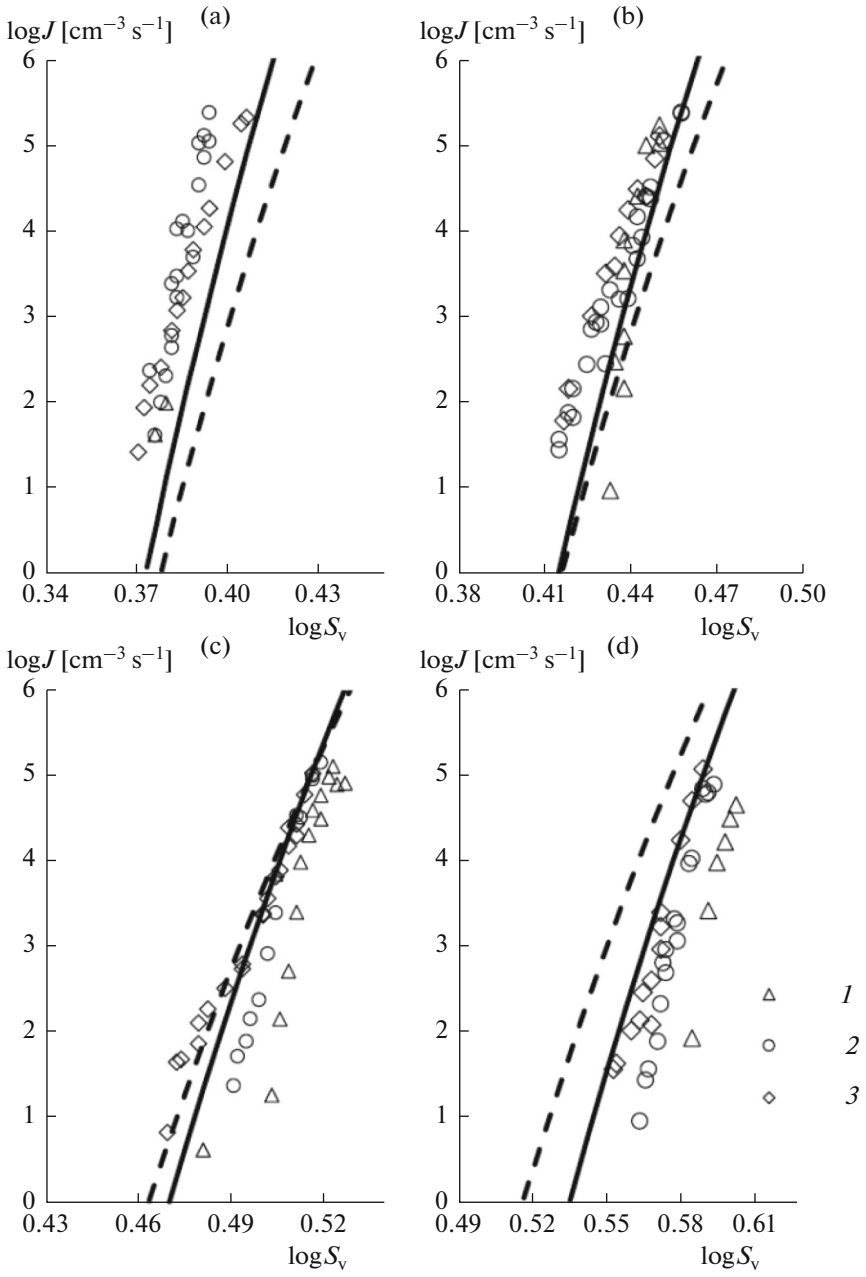

Fig. 6. Dependences of the *n*-propanol nucleation rate on supersaturation plotted by Görke et al. [41] at temperatures of (a) 300, (b) 290, (c) 280, and (d) 270 K and carrier gas pressures of (*1*) 50–60, (*2*) 100, and (*3*) 200 kPa. The data obtained in terms of the proposed theory and the CNT are shown by the solid and dashed lines, respectively.

have been compared with verified experimental data on nucleation in supersaturated vapors of different substances and with predictions of the CNT. The comparison has shown that the sizes of critical nuclei calculated at preset temperature and supersaturation agree with the measured ones and that the nucleation rates obtained in this work either coincide with the measured ones or agree with them within one or two decimal orders of magnitude. The nucleation rates obtained in terms of the proposed theory are in better agreement with experimental data that those found within other versions of the theory.

The accumulation of more accurate and reliable experimental data will make it possible to determine the accuracy of the proposed nucleation theory and suggest methods for its improvement.

ACKNOWLEDGMENTS

We are grateful to A.P. Efimenko for technical support.

APPENDIX

The data of Table 1 are approximated using the following expressions:

(1) for $7 \le \frac{\alpha}{kT} \le 15$

$$\varphi\left(\frac{\alpha}{kT}, g\right) = \frac{g^{2/3}\left(0.56\frac{\alpha}{kT} + 6.65 + 2.3\left(\frac{\alpha}{kT} - 5\right)^{-1}\right)}{\left(g^{1/3} - 1.3\right)^2\left[0.11\left(\frac{\alpha}{kT} - 5\right)^2 + 29.35 - 135\left(\frac{\alpha}{kT} - 20\right)^{-2}\right] + 12\left(g^{1/3} - 1\right) + 30}$$

$$+ \left[0.395 - 0.00082\left(\frac{\alpha}{kT} - 6.5\right)^2 - 0.0085\sin\left(\pi\frac{\alpha - 8kT}{6kT}\right)\right]\sin\left(\frac{\pi g^{1/3}}{13}\right) + \frac{0.01425 - 0.00025\frac{\alpha}{kT}}{\left(g^{1/3} - 1.02\right)^2}$$

$$+ \frac{0.028\frac{\alpha}{kT} + 0.076 - 0.019\sin\left(\frac{\pi}{3.7}\left(\frac{\alpha}{kT} - 6.5\right)\right)}{\left(g^{1/3} - 11\right)^2},$$

(2) for $15 \le \frac{\alpha}{kT} \le 36$

$$\varphi\left(\frac{\alpha}{kT}, g\right) = \frac{g^{2/3}\left(\frac{\alpha^5}{kT} \times 10^{-6} \times 0.208 + 0.215\frac{\alpha}{kT} + 11.7\right)}{\left[\left(g^{1/3} - 0.01662\frac{\alpha}{kT}\right) - 1.067\right]^2\left[38\exp\left(-\frac{\left(\frac{\alpha}{kT} - 20\right)^2}{630}\right) + 40\left(\frac{\alpha}{kT} - 40\right)^{-2}\right] + 12\left(g^{1/3} - 1\right) + 30}$$

$$+ \left[0.442\exp\left(-\frac{\left(\frac{\alpha}{kT} - 10\right)^2}{410}\right) - 0.125\exp\left(-\frac{\left(\frac{\alpha}{kT} - 31.5\right)^2}{24}\right)\right]\sin\left(\frac{\pi g^{1/3}}{14}\right)$$

$$+ \frac{0.029 + 1.05\left(45 - \frac{\alpha}{kT}\right)^{-2} - 0.00111\frac{\alpha}{kT} - 0.03\left(\frac{\alpha}{kT} - 10\right)^{-2}}{g^{1/3} - 1}.$$

REFERENCES

1. Volmer, M. and Weber, A., *Z. Phys. Chem.*, 1926, vol. 119, p. 277.
2. Becker, R. and Döring, W., *Ann. Phys.*, 1935, vol. 24, p. 719.
3. Zel'dovich, Ya.B., *Zh. Eksp. Teor. Fiz.*, 1942, vol. 12, p. 525.
4. Lothe, J. and Pound, G.M., *J. Chem. Phys.*, 1962, vol. 36, p. 2080.
5. Frenkel', Ya.I., *Sobranie izbrannykh trudov* (Selected Works), Moscow–Leningrad: Akad. Nauk SSSR, 1959, vol. 3. Kinetic Theory of Liquids.
6. Feder, J., Russell, K.C., Lothe, J., and Pound, G.M., *Adv. Phys.*, 1966, vol. 15, p. 111.
7. Reiss, H., Katz, J.L., and Cohen, E.R., *J. Chem. Phys.*, 1968, vol. 48, p. 5553.
8. Reiss, H., *J. Stat. Phys.*, 1970, vol. 2, p. 83.
9. Abraham, F.F., *Homogeneous Nucleation Theory*, New York: Academic, 1974.
10. Burton, J.J., in *Modern Theoretical Chemistry*, Berne, B.J., Ed., New York: Plenum, 1977, vol. 5, p. 195.
11. Kuni, F.M. and Rusanov, A.I., *Phys. Lett. A*, 1969, vol. 29, p. 337.
12. Rusanov, A.I. and Kuni, F.M., in *Poverkhnostnye yavleniya v zhidkostyakh* (Surface Phenomena in Liquids), Rusanov, A.I., Ed., Leningrad, 1975, p. 112.
13. Lushnikov, A.A. and Sutugin, A.G., *Usp. Khim.*, 1976, vol. 45, p. 385.
14. Dillmann, A. and Meier, G.E.A., *J. Chem. Phys.*, 1991, vol. 94, p. 3872.
15. Ford, I.J., *J. Mech. Eng. Sci.*, 2004, vol. 218, p. 883.

16. Kodenev, G.G., *Colloid J.*, 2008, vol. 70, p. 589.
17. Kodenev, G.G., Samodurov, A.V., Baldin, M.N., and Baklanov, A.M., *Colloid J.*, 2014, vol. 76, p. 38.
18. Landau, L.A. and Lifshits, E.M., *Statistical Physics*, New York: Pergamon, 1980.
19. Band, W., *Quantum Statistics*, New York: Van Nostrand, 1955.
20. Rusanov, A.I., Kuni, F.M., and Shchekin, A.K., *Kolloidn. Zh.*, 1987, vol. 49, p. 309.
21. Girshick, S.L. and Chiu, C.-P., *J. Chem. Phys.*, 1990, vol. 93, p. 1273.
22. Katz, J.L., Fisk, J.A., and Chakarov, V., Abstracts of Papers, *13 Int. Conf. on Nucleation and Atmospheric Aerosols*, Salt Lake City, 1992, Fukuta, N. and Wagner, P.E.P., Eds., p. 11.
23. Barnard, A.J., *Proc. R. Soc. London A*, 1953, vol. 220, p. 132.
24. Bedanov, V.M., Vaganov, V.S., Gadiyak, G.V., and Kodenev, G.G., *Khim. Fiz.*, 1988, vol. 7, p. 412.
25. Bronshtein, I.N. and Semendyaev, K.A., *Spravochnik po matematike dlya inzhenerov i uchashchikhsya VTUZov* (Handbook on Mathematics for Engineers and Students of Technical High Schools), Moscow: Nauka, 1967.
26. Kodenev, G.G., Preprint no. 3 (Institute of Geology and Geophysics, Siberian Branch, USSR Academy of Sciences, Novosibirsk, 1984).
27. *Spravochnik khimika* (Chemist's Handbook), Nikol'skii, B.P., Ed., Moscow: Khimiya, 1965, vol. 1.
28. Hare, D.E. and Sorensen, C.M., *J. Chem. Phys.*, 1986, vol. 84, p. 5085.
29. Archer, D.G. and Carter, R.W., *J. Phys. Chem. B*, 2000, vol. 104, p. 8563.
30. Viisanen, Y., Strey, R., and Reiss, H., *J. Chem. Phys.*, 1993, vol. 99, p. 4680.
31. Holten, V., Bertrand, C.E., Anisimov, M.A., and Sengers, J.V., *J. Chem. Phys.*, 2012, vol. 136, p. 094507.
32. Bedanov, V.M., Vaganov, V.S., Gadiyak, G.V., Kodenev, G.G., and Rubakhin, E.A., *Khim. Fiz.*, 1988, vol. 7, p. 555.
33. Vaganov, V.S., Kodenev, G.G., and Rubakhin, E.A., Preprint no. 14 (Institute of Geology and Geophysics, Siberian Branch, USSR Academy of Sciences, Novosibirsk: 1985).
34. Rohač, V., Fulem, M., Schmidt, H.-G., Rižička, V., Rižička, K., and Wolf, G., *J. Therm. Anal. Calorim.*, 2002, vol. 70, p. 455.
35. Hrubý, J., Vinš, V., Mareš, R., Hykl, J., and Kalová, J., *J. Phys. Chem. Lett.*, 2014, vol. 25, p. 425.
36. Hämeri, K. and Kulmala, M., *J. Chem. Phys.*, 1996, vol. 105, p. 7696.
37. Mikheev, V.B., Laulainen, N.S., Barlow, S.E., Knott, M., and Ford, I.J., *J. Chem. Phys.*, 2000, vol. 113, p. 3704.
38. Hämeri, K., Kulmala, M., Krissinel, E., and Kodenyov, G., *J. Chem. Phys.*, 1996, vol. 105, p. 7683.
39. Reid, R.C. and Sherwood, T.K., *The Properties of Gases and Liquids*, New York: McGraw-Hill, 1966.
40. Fuks, N.A. and Sutugin, A.G., *Kolloidn. Zh.*, 1964, vol. 26, p. 110.
41. Görke, Neitola, K., Hyvärinen, A.-P., Lihavainen, H., Wölk, J., Strey, R., and Brus, D., *J. Chem. Phys.*, 2014, vol. 140, p. 174301.

Translated by A. Kirilin